

Estimation and Measurement of Alpha Decay Pulses in Fission Detectors and Their Practical Application for Verifying Detector Health

Shigehiro KONO, Masao ISHIKAWA, Shuhei SUMIDA, Michinori YAMAUCHI¹⁾, Daijiro ITO²⁾, Hiroyuki YAZAWA²⁾, Masashi KUROSAKI²⁾, Takashi KOBUCHI³⁾, Kunihiro OGAWA^{3,4)}, Mitsutaka ISOBE^{3,4)} and Yoshihiko NUNOYA

Naka Fusion Institute, National Institutes for Quantum Science and Technology, Naka 311-0193, Japan

¹⁾*NAT Corporation, Tokai 319-1112, Japan*

²⁾*Toshiba Energy Systems & Solutions Corporation, Fuchu 183-8511, Japan*

³⁾*National Institute for Fusion Science, National Institutes of Natural Sciences, Toki 509-5292, Japan*

⁴⁾*The Graduate University for Advanced Studies, SOKENDAI, Toki 509-5292, Japan*

(Received 6 November 2023 / Accepted 30 January 2024)

Signals generated by spontaneous alpha decay of uranium in fission chambers are very small and are buried in background noise. These signals are often simply discriminated by amplitude as unwanted background noise. However, if these signals can be distinguished from white noise, they could function as a checking source that is electric-noise-free and is embedded in the detector itself. To confirm our hypothesis, we estimated and measured the pulse height of alpha decay signals in the fission chambers of the Large Helical Device (LHD) at the National Institute for Fusion Science (NIFS). When background noise was sufficiently low, the plateau curves of alpha decay signals could be measured by using the maintenance function of the neutron monitoring system. When background noise was high, instruments such as an oscilloscope and a multi-channel analyzer (MCA) successfully caught alpha decay signals by using their high-performance trigger functions. Measuring alpha decay pulses is also an indicator of the health of the detector and its preamplifier because if something were wrong with either component, the alpha decay signals would prove difficult to measure. This practical application of alpha decay signals to verify neutron instrumentation systems that use the noise-sensitive Campbelling method will be beneficial for fusion facilities and fission reactors and help meet ALARA policy because this method does not require an external checking source.

© 2024 The Japan Society of Plasma Science and Nuclear Fusion Research

Keywords: alpha decay, fission chamber, Campbelling, neutron instrumentation, fission reactor, LHD, ITER, JT-60SA, BWR

DOI: 10.1585/pfr.19.1405015

1. Introduction

“Will the preamplifier have any control, monitoring, or health-related functions?” was the question from the ITER Organization concerning the Micro Fission Chamber (MFC) system for ITER [1]. Neutron sources such as ²⁵²Cf are usually provided with fission chambers to check the health of detectors and measurement equipment. However, because the MFC detectors of ITER are installed inside a vacuum vessel as shown in Fig. 1, these checking sources cannot be used. Although some preamplifiers are equipped with internal test pulse generators for soundness checking, installing such a signal generator is not ideal because of the electromagnetic noise they would generate. The Campbelling method, used to measure the signals of fission chamber detectors, measures the mean-square voltage (MSV) of small signal fluctuations of a detector [2], and is thus vulnerable to noise. Based on our experience

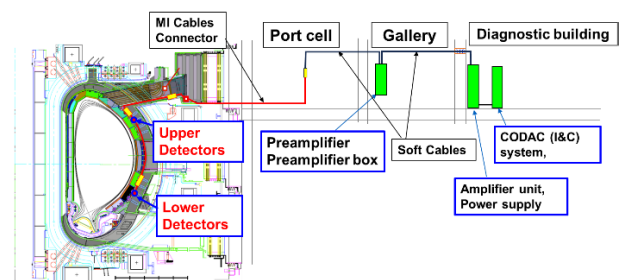


Fig. 1 The MFCs will be installed on the upper (#12) and lower (#17) out-boards behind the blanket modules of the ITER tokamak vacuum vessel.

with neutron monitoring systems for boiling water reactors (BWR), oscillators used for test signals cause noise and affect the soundness of Campbelling measurements. Next, because alpha decay signals do not generate any electric

author's e-mail: kono.shigehiro@qst.go.jp

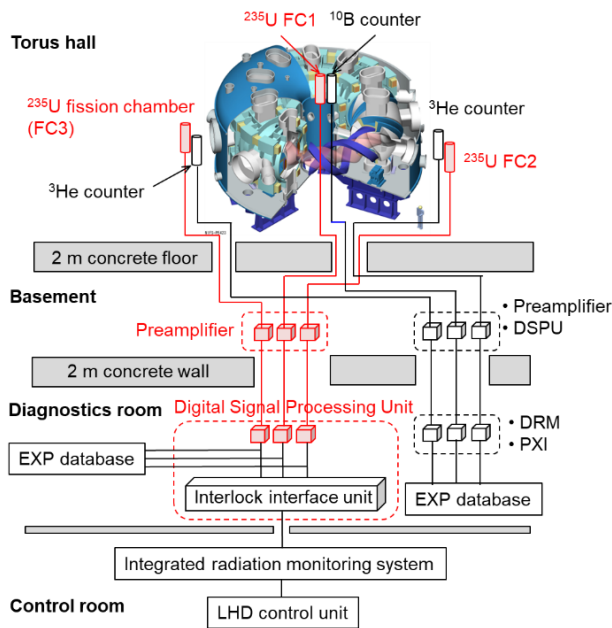


Fig. 2 System configuration of the neutron monitoring system of the LHD.

noise, we focused on the spontaneous alpha decay of uranium coated on the electrodes of fission chambers. However, the average energy of an alpha particle is less than one-tenth the energy of a fission fragment of uranium, and their signals can be easily discriminated and removed from the neutron signals generated by fission fragments. Thus, alpha decay signals are not normally utilized. Alpha decay signals can be measured in good noise conditions, but in high-noise environments the signals are unmeasurable because they get buried in the background noise. The neutron monitoring system that was constructed for the Large Helical Device (LHD) at the National Institute for Fusion Science (NIFS) has good noiseless conditions, therefore we expected to succeed in measuring the alpha decay signals of the fission chambers of the LHD [3,4].

2. Specifications of the Instrument Devices

The neutron monitoring system of the LHD consists of three sets of ²³⁵U fission chamber detectors, preamplifiers, and digital signal processing units [5]. The configuration of the system is shown in Fig.2 [3]. The signals generated by the spontaneous alpha decay of uranium coated on the electrodes of fission chambers were measured at the input to the digital signal processing unit; the fission chambers and preamplifiers were the main contributors for measuring the alpha signals. The specifications of the fission chambers and preamplifiers are shown in Table 1 and Table 2, respectively. The cable lengths between them are shown in Table 3.

Table 1 Specifications of the fission chamber detectors.

Item	Specification
Model Number	KSA-01 [6]
Fissile Material	UO ₂ 300 mg (²³⁵ U)
Filler Gas	Ar/N ₂ 787 kPa[abs]
Thermal Neutron Sensitivity	0.1 s ⁻¹ /(s ⁻¹ ·cm ⁻²)
Charge Accumulation Time	80 ns
Maximum Operating Voltage	400 VDC
Detector Capacitance	approx. 155 pF
Size	339 mm × 28 mm φ

Manufacturer: Canon Electron Tubes & Devices
(Formerly Toshiba Electron Tubes & Devices)

Table 2 Specifications of the preamplifiers.

Item	Specification
Model Number	HNA400
Maximum Input Signal	50 mVpp
Gain	40.5 dB
Passing Band	100 kHz – 10 MHz
Maximum Output Signal	1 Vpp
Maximum Detector Bias Voltage	400 V
Maximum Detector Current	10 mA
Size	116 mm(H) × 292 mm(W) × 192 mm(D)

Manufacturer: Toshiba Energy Systems & Solutions Corporation

Table 3 Signal cable lengths of the neutron monitoring system.

From	To	Length
FC1	Preamplifier	35 m
FC2	Preamplifier	52 m
FC3	Preamplifier	50 m
Preamplifiers	Digital signal processing units	95 m

3. Estimation

The fission chamber detectors used in the LHD have only ²³⁵U as their fissile material. The amount of UO₂ is about 300 mg, so the number of ²³⁵U atoms is 6.76 × 10²⁰. The half-life of ²³⁵U is 7.08 × 10⁸ years, so the decay constant of ²³⁵U is 3.12 × 10⁻¹⁷ s⁻¹. Therefore, the decay rate is 2.11 × 10⁴ s⁻¹. Because uranium is coated on the inner surface of the outer electrodes of the fission chambers and alpha particles are emitted toward both the inside and outside of the electrode, the detection efficiency was estimated to be 50%. Therefore, the expected counting rate of the pulses generated by the spontaneous alpha decay of

^{235}U coated on the electrodes of the fission chambers is 1×10^4 counts per second (hereinafter referred to as cps).

The maximum amplitude of the signal pulses generated in the fission chambers was calculated based on [2] and [7].

Assuming that the specific energy loss of the alpha particles in argon gas is equivalent to that of air, the range of the alpha particles in argon gas was estimated from the range in air, that is $R = 0.318E^{3/2}$ [8]. Considering the density of argon gas, 1.783 kg/m^3 , the energy of the alpha particles at position x cm on the track is shown below.

$$E = (E_1^{3/2} - P \cdot x/0.178)^{2/3}. \quad (1)$$

Here, P is the argon gas pressure at 0°C .

From Eq. (1), the range of the alpha particles, which have an average energy of 4.4 MeV , was calculated as 2.1 mm in argon gas pressurized to 787 kPa , which is the filler gas pressure of the fission chambers.

Equation (2) was used to calculate the energy of fission fragments, assuming that the specific energy loss of the fission fragments in argon gas is also equivalent to that of air [9].

$$E = (E_1^{2/3} - P \cdot x/0.0785)^{3/2}. \quad (2)$$

From Eq. (2), the range of light fission fragments having an energy of 93 MeV was calculated as 2.1 mm , and the range of heavy fission fragments having an energy of 67 MeV was calculated as 1.7 mm in argon gas pressurized to 787 kPa .

The flight lengths of the alpha particles and the fission fragments were calculated considering the dual-cylinder structure of the fission chamber detectors. The inner electrode radius (r_1) was 10.5 mm and the outer electrode radius (r_2) was 11 mm , thus an electrode gap of 0.5 mm . When a detector is cut obliquely at an angle φ , the cross section will be a dual ellipse. When a particle is emitted from point P on the outer ellipse (the negative electrode) in a direction having angle θ , the particle will reach the inner ellipse (the positive electrode) at distance X_1 . The particle will reach another point on the outer ellipse at distance X_2 in the case that θ is larger than the following angle as shown in Fig. 3.

$$X_1 = \{r_2 - [r_2^2 - (\tan^2 \theta \cos^2 \varphi + 1)(r_2^2 - r_1^2)]^{1/2}\} / (\tan^2 \theta \cos^2 \varphi + 1) \times (\tan^2 \theta + 1)^{1/2}. \quad (3)$$

When $\theta > \tan^{-1}(r_1 / \cos \varphi \times 1 / (r_2^2 - r_1^2)^{1/2})$

$$X_2 = 2r_2 / (\tan^2 \theta \cos^2 \varphi + 1) \times (\tan^2 \theta + 1)^{1/2}. \quad (4)$$

The energy loss of particles in argon gas was calculated by subtracting the energy at X_1 or X_2 , which was calculated by Eq. (1) for the alpha particles or by Eq. (2) for the fission fragments, from the initial energy E_1 . When X_1 or X_2 is longer than the range of the particles, the particles will lose all of their initial energy in argon gas.

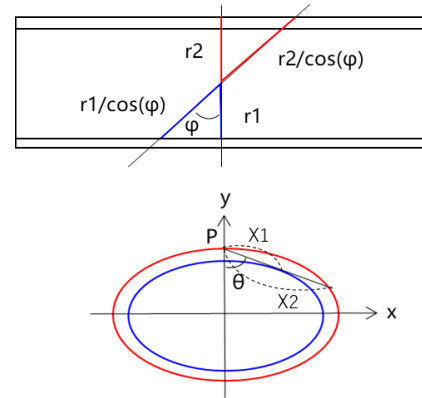


Fig. 3 Flight length calculation in a dual-cylinder electrode detector.

The energy loss in argon gas was divided by a W -value of 26.3 eV , the average energy lost by the alpha particles per ion pair formed in argon gas [10], to obtain the electric charge (Q_0) created by the ionization of argon gas. Columnar recombination was used to estimate the electric charge (Q) acquired at the electrodes based on Eq. (5) and the values reported in Ref. [11].

$$Q/Q_0 = \ln(1 + \kappa \cdot k/b) / (\kappa \cdot k/b), \quad (5)$$

where,

$k/b = 2.5 \times 10^{-5} \text{ m}^2/\text{s}$ when electrode distance is 0.5 mm ,
 $\kappa = 1.52 \times 10^5 \text{ s/m}^2$ for 4 bar gas pressure and 200 V bias,

also

$$\kappa = C \cdot X_0(1\text{bar}) \cdot d \cdot P^2 / (\pi \cdot (\mu_e + \mu_a)(1\text{bar}) \cdot \Delta V). \quad (6)$$

To calculate Q/Q_0 for gas pressure P (bar) and bias V (V), Eq. (7) was used with converted κ' .

$$Q/Q_0 = \ln(1 + \kappa' \cdot k/b) / (\kappa' \cdot k/b), \quad (7)$$

where,

$$\kappa' = \kappa \cdot (P/4)^2 / (V/200). \quad (8)$$

The maximum detector current was calculated based on the assumption that the ionization of argon gas occurs equivalently along the track of the fission fragments and the alpha particles, and the generated electrons move to the anode with a constant velocity of W_e when derived by the electric field. The following formula was used for the calculation because the preamplifiers of the LHD are electric-current pulse amplifiers having a time constant τ_0 that was shorter than the electron collection time T_e . A cable terminated with a specific impedance r_0 has an impedance r_0 when viewed from the sending end. Therefore, unlike charge

amplifiers, there is no need to consider the cable capacitance for this current pulse preamplifier even if the cables are lengthened [12].

$$I_{\max} = Q_e/T_e[1 - \exp(-T_e/\tau_0)], \tag{9}$$

where,

$$Q_e = Q,$$

$$T_e = d/T_e.$$

In the case of KSA-01 detectors,

- T_e : electron collection time; 80 ns
- τ_0 : time constant; input impedance (r_0)
× detector capacitance (Cd)
- r_0 : 75 Ω
- Cd: 155 pF

Finally, the pulse voltage was calculated by multiplying the maximum current by the input impedance (75 Ω), the preamplifier gain ($\times 100$), and the amplifier gain ($\times 20$).

Figure 4 shows the calculated pulse height distribution of signals generated by the alpha particles and the fission fragments in a KSA-01 detector biased with 300 V.

When a light fragment loses all its initial energy of 93 MeV in argon gas, it creates a pulse at 736 mV. When a heavy fragment loses an energy of 67 MeV, it creates a pulse at 530 mV. With the exception of these peaks, the mode of the pulse height distribution of the fission fragments exists between 250 - 260 mV owing to the narrow gap between electrodes. The mode of the alpha pulses also exists between 0 - 10 mV, which is nearly the same level as that of white noise. The lowest pulse height of the alpha decay signals is 5.7 mV, which corresponds to the case where an alpha particle flies the shortest distance between the electrodes, i.e., 0.5 mm.

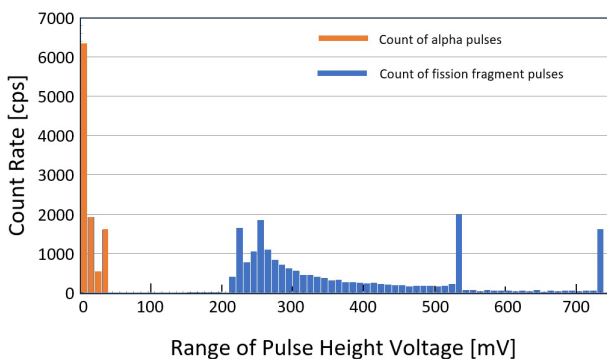


Fig. 4 Histogram of the pulse height distribution of a KSA-01 fission chamber at $P = 787$ kPa and $V = 300$ V. Alpha count rate (red) = 1×10^4 cps, neutron (fission fragments) count rate (blue) = 1×10^4 that is only for simulation. (Note: the actual count rate depends on the strength of the neutron source.)

4. Measurement

We had a high expectation of success in measuring the alpha decay pulses, even in a currently operational facility having long signal cables as shown in Table 3, because the current pulse preamplifier is used in the LHD. Two types of data were acquired to obtain information from alpha decay pulses. One was the equipment maintenance data including the discrimination characteristics and the plateau characteristics, which were functions installed in the digital signal processing unit. The other was the raw data of the output signal from the preamplifier, which was acquired using an oscilloscope (Tektronix, Inc, model: MSO64). The signal level of the raw data measured by the oscilloscope was one-twentieth the level of the equipment maintenance data, because the input signal amplifier of the digital signal processing unit multiplied the input signal by 20. The configuration of the measurement circuit and the measurement setup are shown in Fig. 5 and Fig. 6, respectively.

4.1 Measurement in a low noise channel

First, the measurements in a low noise case are explained.

Pulse plateau characteristics of fission chamber No. 3 (FC3) located at 4-O were measured at a discrimination level of -100 mV by using a function of the digital signal processing unit. Figure 7 shows the pulse plateau characteristics of FC3.

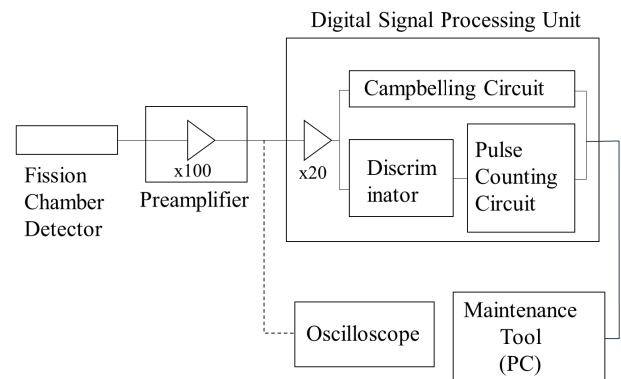


Fig. 5 Configuration of the measurement circuit.



Fig. 6 Photo of the measurement setup. A plain stitch wire for the earthing of the signal earth was used.

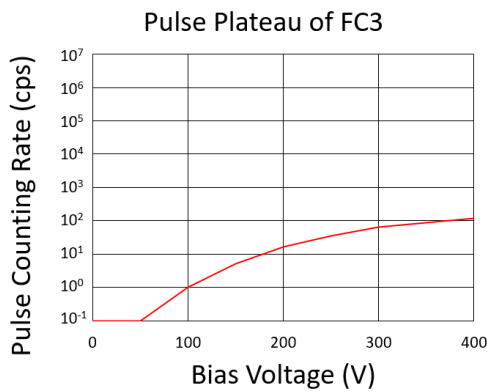


Fig. 7 Pulse plateau characteristic curve of FC3. The range of the bias voltage for FC3 was 0 - 400 V. The measurement time at each bias voltage was 60 s. The interval of the bias voltage was 50 V. The discrimination voltage was set to -100 mV. (hereinafter these parameters are expressed as: range = 0/400 V, interval = 60 s, step = 50 V, dscrm = -100 mV)

As can be seen in Fig. 7, the plateau curve of FC3 had an ideal plateau curve: the counting rate starts from 0 cps at a bias voltage of 0 V and it has a saturation curve over 50 V. This indicates good signal/noise (S/N) conditions in which the noise level is low and the alpha pulse height is high enough to distinguish the alpha pulses from the noise.

The discrimination characteristics of FC3 were measured with detector biases of 0 V or 300 V by using a function of the digital signal processing unit as shown in Fig. 8. A swelling on the discrimination line was observed in the discrimination characteristics of FC3 biased by 300 V. The swelling was created by the alpha pulses, which were expected before measurements were performed.

The discrimination curves show the integrated values of the number of pulses higher than the discrimination level, therefore, the derivative of the discrimination curve provides the pulse height distribution. The derivative of Fig. 8 (b) was subtracted from that of Fig. 8 (a) to obtain the pulse height distribution of the alpha decay signals only, removing noise data. Figure 9 shows the calculation results. The zone hatched in gray was not considered because the error of the count rate was large due to background noise. The peak of the pulse height distribution of the alpha decay signals was read out as -50 mV from Fig. 9. This value was 8.8 times larger than the expected value of -5.7 mV, which was calculated in Sec. 3 and considered the preamplifier gain (100 times) and the input gain of the digital signal processing unit (20 times).

4.2 Measurement in a high noise channel

Next, the measurements in the high noise case are explained. The discrimination characteristics were also measured in fission chamber No. 2 (FC2) located at 10-O. In this case, the discrimination characteristics of FC2 did not

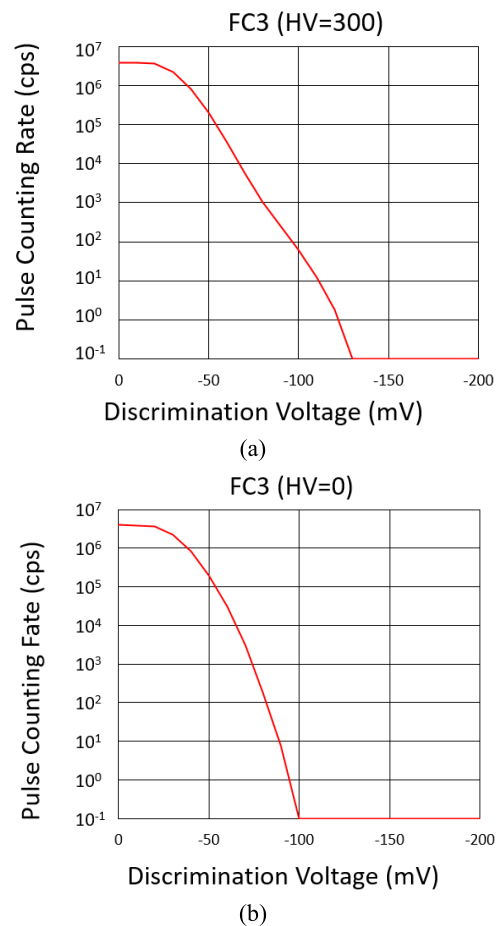


Fig. 8 Discrimination characteristic curves of FC3. (range = 0/-200 mV, interval = 60 s, step = 10 mV, bias voltage (HV) = (a) 300 V/(b) 0 V)

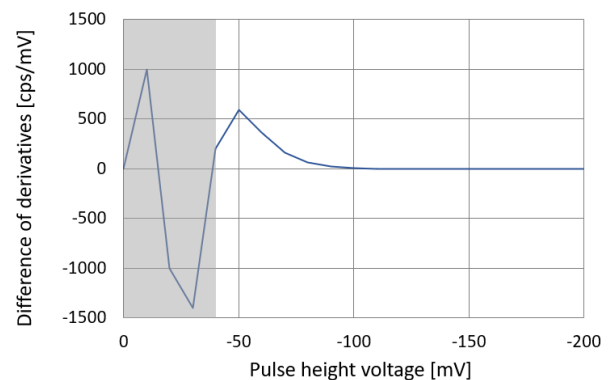


Fig. 9 Difference between the derivatives of Fig. 8 (a) and (b), which indicates the pulse height distribution of the alpha decay signals except for the zone hatched in gray where the count rate error was large due to background noise.

show any difference between the detector biases of 0 V or 300 V as shown in Fig. 10.

When the pulse plateau characteristics were measured, the plateau curve was initially a flat line, as shown in Fig. 11.

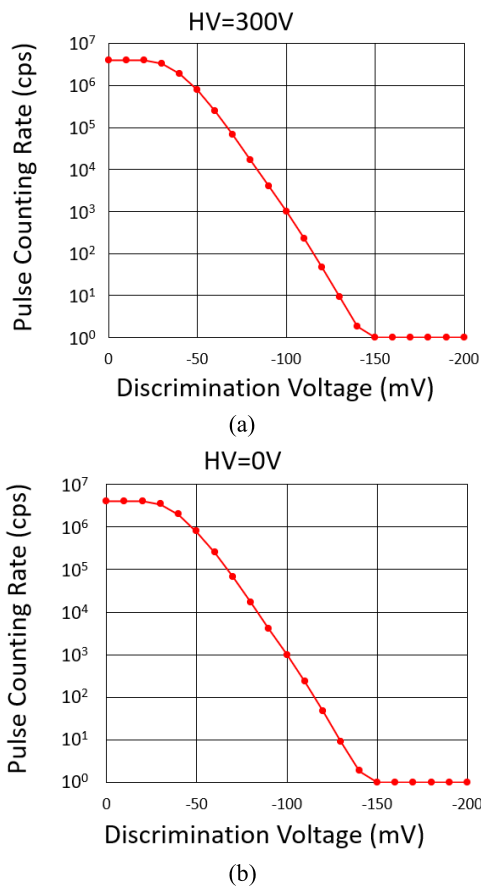


Fig. 10 Discrimination characteristic curves of FC2. (range = 0/−200 mV, interval = 60 s, step = 10 mV, HV = (a) 300 V/(b) 0 V)

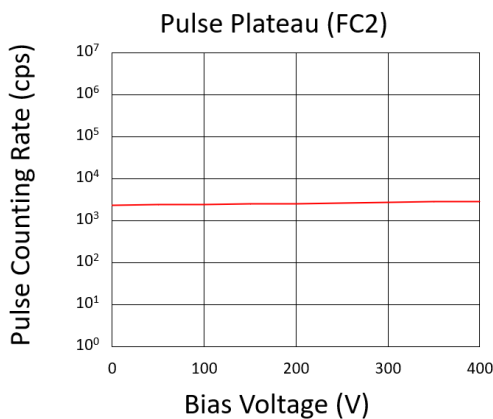


Fig. 11 Pulse plateau characteristic curve of FC2. (range = 0/400 V, interval = 60 s, step = 50 V, dscrm = −100 mV)

The input signal cable was removed from the digital signal processing unit so that the pulse plateau characteristics could be measured without the input signals, after which, the counting rate at each bias voltage was 0.

Because a loose input signal connection might be the cause of noise, the input signal connector on the rear panel

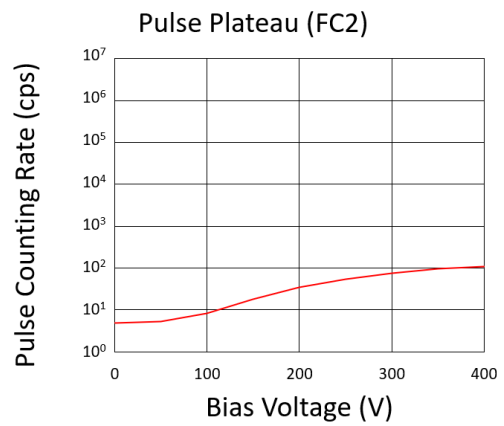


Fig. 12 Pulse plateau characteristic curve of FC2 after connector mating/unmating. (range = 0/400 V, interval = 60 s, step = 50 V, dscrm = −100 mV)

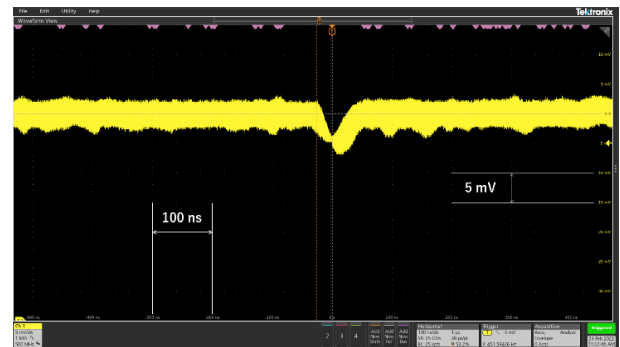


Fig. 13 Alpha pulse shape triggered with −5 mV when FC2 was biased by 300 V [Horizontal Scale: 100 ns/div, Vertical Scale: 5 mV/div, hereinafter, the oscilloscope’s scales are the same except for Fig. 15].

of the digital signal processing unit was repeatedly mated and unmated to decrease contact noise, after which, the plateau curve improved slightly, as shown in Fig. 12.

In this case, it was shown that the alpha signals were small and easily buried in the background noise, therefore, noise mitigation was crucial in measuring the alpha signals.

4.3 Direct measurement of the alpha decay signals

After the measurement shown in Fig. 12, to confirm the noise conditions in FC2, the output signals from the preamplifier for FC2 were directly observed by an oscilloscope having a storage mode with a trigger level of 5 mV. Even in high-noise conditions such as FC2, the oscilloscope was able to catch the alpha decay signals. Figure 13 shows the waveform of the pulses generated by the spontaneous alpha decay of ²³⁵U coated on the electrodes of FC2 when the detector was biased at 300 V.

The measured average alpha pulse height was 5.7 mV,

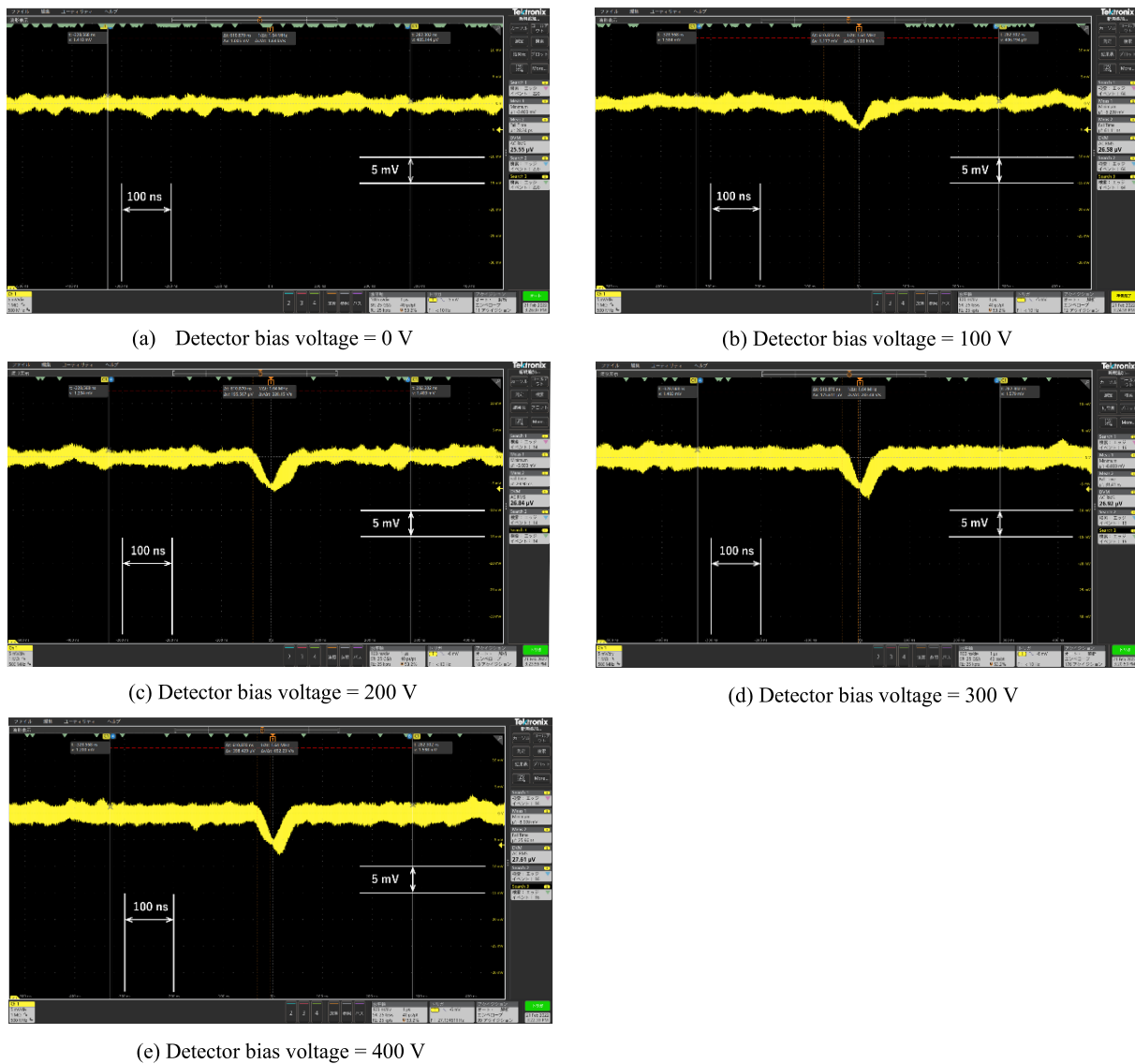


Fig. 14 Pulse shapes of the alpha decay signals captured by the oscilloscope when FC3 was biased by 0 V (a) to 400 V (e).

and the average noise amplitude was approximately 4 mV, which explains why the discrimination characteristics cannot distinguish the alpha signals from the noise. The oscilloscope screen indicated that the trigger frequency was 451 Hz (i.e., cps), which corresponded to the pulse counting rate at -103 mV in the discrimination voltage shown in Fig. 10 (a).

Under good noise conditions, the waveforms of FC3 captured in the same manner as FC2 were depicted more clearly than those of FC2. The results are shown in Fig. 14 (a) through (e). The pulse heights of the alpha signals are higher than the noise level. The alpha pulse heights vary depending on the detector bias voltage. The alpha pulses were obtained at detector bias voltages of 0 V, 100 V, 200 V, 300 V, and 400 V, and are summarized in Table 4. Note that 0 V bias indicates the noise level. The noise levels of FC3 were approximately half the noise levels of FC2 when the detectors were biased, even though these noise levels were the same when the detectors were not biased.

The signal level of the alpha decay pulses measured by the oscilloscope was also higher than those of Sec. 3.

5. Discussion

5.1 Measurement of the neutron pulse signal

The pulse signals generated by the alpha decay could be monitored in the LHD, a currently operational facility, which begs the question of why the pulse heights of the alpha decay signals were larger than those of the estimation. Firstly, it was suspected that the preamplifier gains between the calculation and the actual equipment were different. To confirm this, further data were acquired by using a ^{252}Cf checking source to obtain the neutron pulse signals.

Figure 15 shows a screen capture of the oscilloscope that displayed the pulse waveforms of KSA-01 detectors exposed to ^{252}Cf and biased at 300 V.

Table 4 summarizes the measured values and the multiplied values of the measurements by 20, which was the

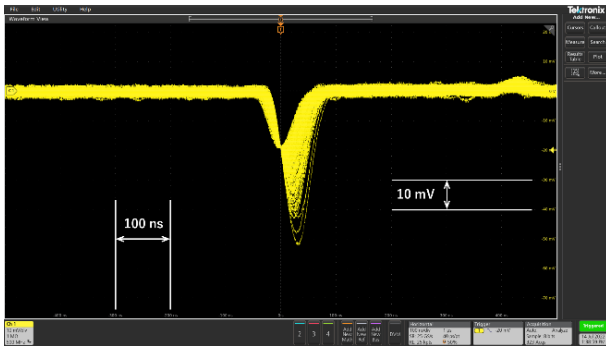


Fig. 15 Screen capture of the oscilloscope when FC3 was exposed to ²⁵²Cf and biased at 300 V [Horizontal Scale:100 ns/div, Vertical Scale:10 mV/div].

Table 4 Pulse height voltages of the decay alphas and the fission fragments of KSA-01 detectors measured in the preamplifier output and signal levels multiplied by 20.

Bias [V]	Measured pulse height [mV]		20 times multiplied value [mV]	
	Decay α	Fission fragments	Decay α	Fission fragments
0	±2	±3	±40	±60
100	3 - 5	8 - 16	60 - 100	160 - 320
200	4 - 6	13 - 32	80 - 120	260 - 640
300	5 - 7	19 - 52	100 - 140	380 - 1040
400	5 - 8	23 - 52	100 - 160	460 - 1040

gain of the input circuit of the digital signal processing unit. The multiplied values correspond to the signal levels of the discrimination and the plateau characteristics. In Table 4, the alpha decay pulses are distributed between 100 - 140 mV and the fission fragments pulses are distributed between 380 - 1040 mV, when the detector is biased at 300 V.

5.2 Measurement of pulse height distribution by MCA

Figure 16 shows the pulse height distribution of KSA-01 detectors measured by a multi-channel analyzer (TechnoAP, APV8104-14LW) having a waveform selector. The pulse height is calculated based on the integrated area of the pulse. In Fig. 16, channel 8000 corresponds to 1 V. The highest peak around channel 1300 (corresponding to 160 mV) in Fig. 16 indicates the peak of the alpha decay signals. This value (160 mV) was slightly higher than that measured by the oscilloscope and multiplied by the input circuit gain shown in Table 4. At the time the measurements were performed by the MCA, background noise was included in the integrated area to calculate the pulse height. Because the ²⁵²Cf used was not strong, the statistical error of the measurement of the pulses created by the fission

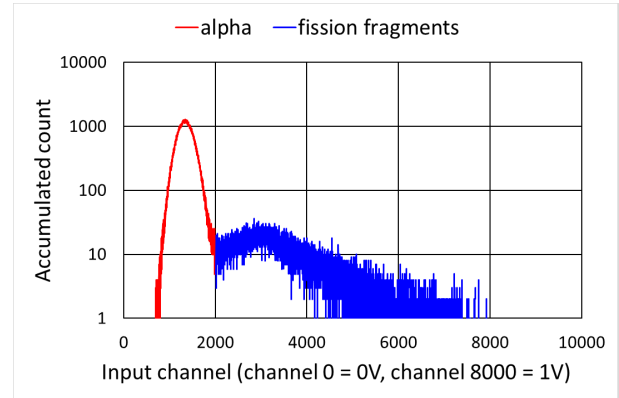


Fig. 16 Pulse height distribution of a KSA-01 detector exposed to a ²⁵²Cf neutron source. These data were measured by an MCA having a pulse shape selection function.

fragments in channels 3000 to 8000 (corresponding to 375 - 1000 mV) was large. However, the pulse height range of the fission fragments almost equals the value measured by the oscilloscope at the 300 V bias, as shown in Table 4. Therefore, the preamplifier gain used in the calculation was changed from 100 to 150 based on the values measured by the oscilloscope and the MCA so as to equalize the neutron pulse height distribution of the calculation with that of the measurements.

5.3 Calculation of the stopping power of alpha particles in Ar gas

Even after changing the preamplifier gains in the calculation, the pulse heights of the alpha decay signals were still lower than those of the measurements. Therefore, the stopping power of argon gas for 4.4 MeV alpha particles, which is the average energy of the decay alphas of ²³⁵U, was calculated by using the Bethe-Bloch formula [13] to re-evaluate the pulse heights of the alpha decay signals. Figure 17 shows the calculated specific energy loss of the alpha particles in argon gas.

The calculated curve was overlaid with the function of $11.724/E^{1.1}$. Consequently, Eq. (10), which shows the energy of the alpha particles as a function of position x , was obtained assuming that E_1 was the initial energy of the alpha particles.

$$E = (E_1^{2.1} - P \cdot x/0.02278)^{1/2.1}, \tag{10}$$

where

P is gas pressure converted to standard gas conditions at 0°C.

From Eq. (10), the range of 4.4 MeV alpha particles in argon gas at 787 kPa was calculated as 0.66 mm.

In Fig. 18, which was re-calculated using this range (0.66 mm), the mode of the pulse height distribution of the alpha decay signals fell between 50 - 60 mV, which was

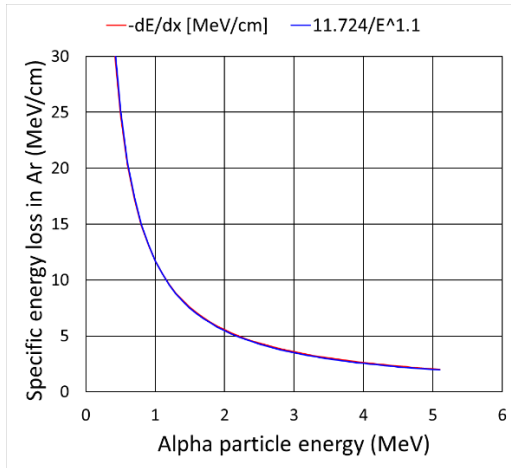


Fig. 17 Specific energy loss of the alpha particles in Ar gas calculated by the Bethe-Bloch formula.

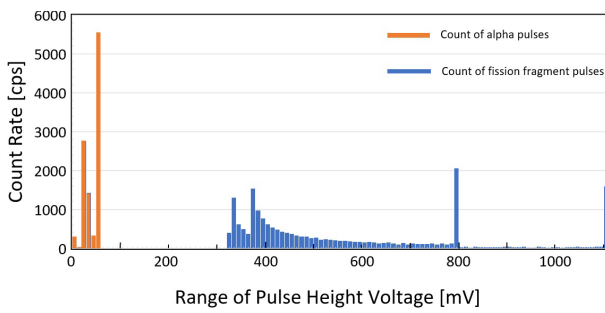


Fig. 18 Histogram of the pulse height distribution of a KSA-01 fission chamber at $P = 787$ kPa and $V = 300$ V, using the re-calculated range of 4.4 MeV alpha particles in Ar gas. The preamplifier gain was set to 150 for this and subsequent calculations.

slightly closer to the measurement. Even though this value met the rough calculation in Fig. 9, the pulse height voltages of the alpha decay signals of Table 4 were still two to three times those of the values of Fig. 18.

5.4 Re-consideration of the columnar recombination rate of the alpha particles

The pulse height voltage of 50 - 60 mV in Fig. 18 corresponds to the case in which the alpha particles completely lose their energy of 4.4 MeV in argon gas. If the columnar recombination rate of the alpha particles is smaller than that of the fission fragments, the pulse heights of the alpha decay signals would be slightly higher and still be closer to those of the fission fragments. As described in [2], the recombination rate is proportional to the product of the concentrations of the two species involved. In fission chambers, ionization is produced along the track of the fission fragments or the alpha particles, and the density of the ionization products is proportional to the energy loss of the particles. In the shortest distance between the elec-

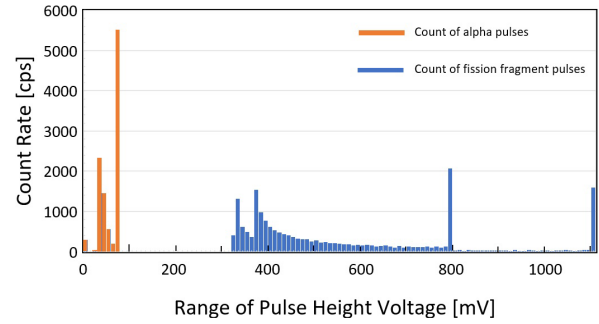


Fig. 19 Histogram of pulse height distribution reconsidered for the recombination rate.

trodes, the light fission fragments lose 27.8 MeV, the heavy fission fragments lose 31.5 MeV, and the alpha decay particles lose 2.2 MeV. When the recombination rate of the decay alphas is calculated as the rate of energy loss, i.e., the energy loss of the alphas divided by the average of the energy loss of the fission fragments, the pulse height distribution is as shown in Fig. 19. The highest pulse height of the alpha decay signals becomes 73.7 mV, which is half of the measured pulse height of the alpha decay signals.

5.5 Consideration of self-shielding by uranium coated on the negative electrodes

Because the two peaks indicated at the right side of the pulse height distribution in Fig. 19 were not observed by the MCA as shown in Fig. 16, self-shielding by the uranium layer coated on the negative electrodes of the fission chambers was examined.

When fission fragments or alpha particles are emitted from the inside of the uranium layer coated on the negative electrodes, these particles lose their energy inside the uranium layer. The energy losses in the uranium layer were calculated in the same way as those in argon gas, i.e., by using stopping powers calculated by the Bethe-Bloch formula (assuming that this formula can be applied to the uranium layer). Equation (11) provides the energy of the particles at distance x from the point of emission.

$$E = (E_0^{2.05} - 2.05 \cdot a \cdot x)^{1/2.05}, \quad (11)$$

where

“ E_0 ” is the initial energy, 93 MeV for light fission fragments, 67 MeV for heavy fission fragments, and 4.4 MeV for decay alphas.

Coefficient “ a ” is 1.89×10^9 for light fission fragments, 5.19×10^9 for heavy fission fragments, and 50000 for decay alphas.

When $E=0$ in Eq. (11), x provides the range of an emitted particle in the uranium layer. The range of the light fission fragments was calculated as $2.8 \mu\text{m}$ and that of the decay alphas was $203 \mu\text{m}$. These ranges are longer than the $1\text{-}\mu\text{m}$ -thick uranium layer, so these particles could fly out

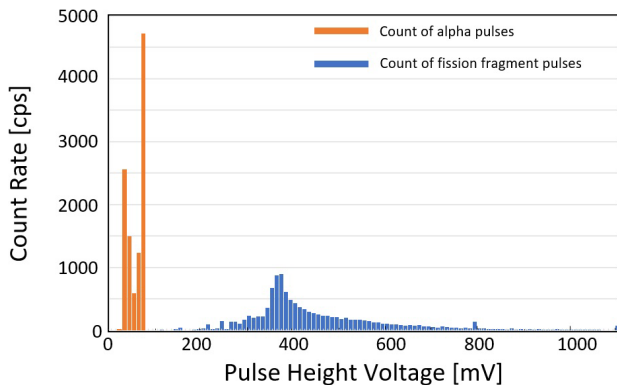


Fig. 20 Histogram of pulse height distribution taking into consideration self-shielding by uranium.

from the uranium layer even though they lost some of their energy in the uranium layer. The range of the heavy fission fragments was calculated as $0.52\ \mu\text{m}$, which is shorter than the thickness of the uranium layer. Therefore, half of the heavy fission fragments could not fly out from the uranium layer. Even if the heavy fission fragments could fly out from the uranium layer, the particles would have lost significant energy in the uranium layer. The heavy fission fragments emitted from the middle of the uranium layer may fly out into argon gas having small energies and create ionized pulses similar to those of the decay alphas. We considered this to be the cause of the difference between the results measured by oscilloscope (Table 4) and by MCA (Fig. 16). The fission chambers were not irradiated by a ^{252}Cf checking source in the measurements by oscilloscope, however, the fission chambers were irradiated in the measurements by MCA. A slight shift in the pulse height distribution of the alpha pulses to a higher voltage was also observed by the MCA when the fission chambers were irradiated by the ^{252}Cf checking source.

The pulse height distributions were calculated by changing the depth of the emission points from $0\ \mu\text{m}$ (i.e., on the surface of the uranium layer) to $1\ \mu\text{m}$ (i.e., on the bottom of the uranium layer) every $0.05\ \mu\text{m}$ step. Figure 20 shows a summation of the 21 results of these pulse height calculations. The peaks at the right side of the pulse height distribution became smaller in Fig. 20, with the highest pulse height of the alpha decay signals being $72.2\ \text{mV}$.

6. Application of the Alpha Decay Signals

As confirmed in Sec. 4, the signals generated by the spontaneous alpha decay of the uranium coated on the electrodes of the fission chambers were observable in a system in a currently operational facility having long cables between the detectors and preamplifiers. In contrast, in a laboratory setting, short cables are usually used to mitigate the influence of noise because charge-sensitive preamplifiers are used to measure the alpha decay signals. It can be

said that the use of an electric-current pulse preamplifier made the measurement of the alpha decay signals possible in the LHD, therefore, facilities that use the same type of preamplifier for their fission chambers can measure the alpha decay signals.

Alpha decay pulses can be an indicator of measurement system health, i.e., verify that the components of a system are functioning properly. If something were wrong with any component in the system, the alpha decay signals could not be observed because they would be small and difficult to measure.

A discrimination circuit is used to distinguish the neutron signals from the other signals. For this purpose, the discrimination level is set at the x-intercept of the extension line of the slope of the noise portion in a discrimination curve, which is around $-150\ \text{mV}$ in Fig. 10. When the noise level is mitigated lower than the pulse height of the alpha decay signals, the discrimination level can be set at the highest noise level to distinguish the alpha decay signals from the noise. The discrimination level was evaluated at $-100\ \text{mV}$ comparing Figs. 8 (a) and (b) in the case of the LHD. The plateau characteristics measurements, usually provided by neutron measurement equipment as a basic maintenance function, can be used to easily verify the health of the detectors and the preamplifiers. The plateau characteristics should show an ideal curve, as shown in Fig. 7, and the pulse count rate should be stable under the same noise conditions. Changes to the shape of the plateau curve or the pulse count rate of the alpha decay signals from the initial conditions may indicate that the detectors or the preamplifiers are not functioning properly. Thus, when such changes are detected, these components should be thoroughly checked.

However, when the noise level is higher than the alpha decay pulses, the plateau characteristics will indicate a semi-flat line, as shown in Fig. 11. Even in such noise conditions, an oscilloscope equipped with a high-performance trigger function can catch the alpha pulses provided that the neutrons can be measured. The oscilloscope can pick up the alpha pulses directly in the signals from the preamplifier by using several trigger settings, such as the falling-edge trigger with an adequate trigger level (e.g., $5\ \text{mV}$). An MCA equipped with a waveform-selection function, such as the pulse rise time (e.g., $80\ \text{ns}$) and the pulse width (e.g., $200\ \text{ns}$), can also catch alpha pulses. The pulse height and the pulse height distribution of the alpha decay signals initially recorded under good conditions will be compared with subsequent measurements, and if any changes are detected, a more detailed investigation will be performed. The same is true in the case of the plateau curve. If the noise conditions are insufficient to measure the neutron signals, the noise conditions should be improved first.

General methods for verifying the soundness of detectors and preamplifiers in detail are as follows. External equipment such as a pulse generator or a function generator can be used to verify the gain of the preamplifier, the

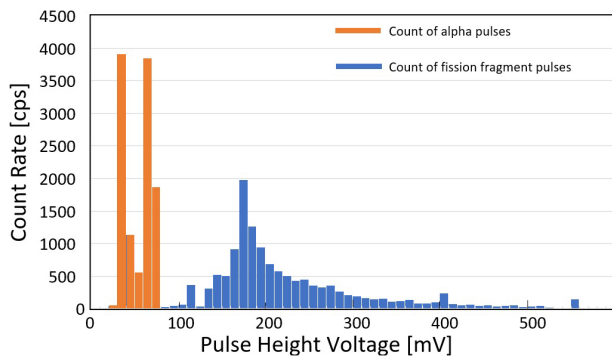


Fig. 21 Histogram of the pulse height distribution of the micro fission chamber for ITER.

linearity of the gain, and the frequency characteristics. For detectors installed in inaccessible areas, the methods for detailed verification are limited. A decrease in the pulse height indicates either a leak of detector gas or an increase in the conductivity of the cables or the connectors. Increased unexpected pulses may occur when the insulation resistance of the detector or the cables deteriorates. In such cases, measuring the insulation resistance will provide information about the defect. Connector tapping may also be useful to check for a bad contact in the connector.

A method to check the health of the fission chamber detectors and the preamplifiers without having to use an external checking source is convenient especially when the detectors are set in a place that people cannot access. Even if the detectors are located in an accessible area, this method helps meet the ALARA policy of avoiding exposure to radiation as low as reasonably achievable.

In the case of the Micro Fission Chamber (MFC) system of ITER, detectors are installed inside the vacuum vessel of the tokamak where people cannot access the detectors because the materials will become radioactive after DD or DT plasma operations. Even in such cases, the health of the detectors and the preamplifiers can be verified when the ionizing reaction in the detectors and the signal amplification by the preamplifiers are confirmed by plateau measurements and by observing the alpha pulses via oscilloscope or MCA. Figure 21 shows the calculated pulse height distribution of the micro fission chamber (200 mm \times 14 mm ϕ) for ITER. The pulse heights of the fission fragments are calculated to be lower than those of the KSA-01 detectors because the electrode gap of the micro fission chamber for ITER is narrower than that of KSA-01. However, the largest pulse height of the alpha decay signals is estimated to be 70.1 mV, which is almost the same as KSA-01. Hence, the measurement of the alpha decay signals is expected to be possible in ITER, although the cable lengths between the micro fission chambers and the preamplifiers is approximately 30 m and between the preamplifiers and the signal processing units is at maximum 150 m.

This method was used to test a neutron monitoring

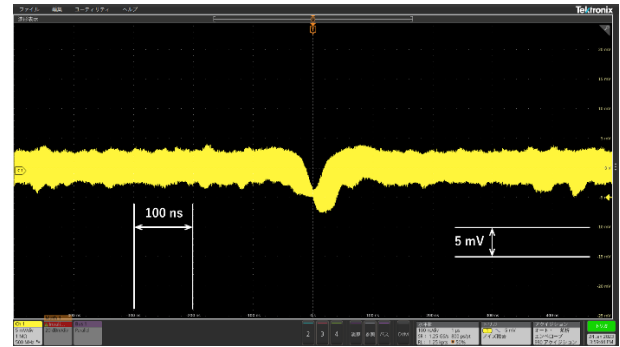


Fig. 22 Pulse shape of the alpha decay signals measured in JT-60SA.

system having fission chambers in JT-60SA at QST in Japan, which facilitated the management of operations by not having to use an external neutron source. The types of fission chambers and preamplifiers of JT-60SA are the same as those of the LHD. In JT-60SA, the cable length between the fission chambers and the preamplifiers is 5 m and between the preamplifiers and the signal processing units is 50 m. This method contributed to resolving noise issues, and the alpha decay signals were measurable by oscilloscope. Figure 22 shows the pulse shape of the alpha decay signals measured in JT-60SA, even though the noise level was high, the results are approximate to those of FC2 in the LHD.

Furthermore, if this method can be applied to the verification of the Startup Range Neutron Monitor (SRNM) system of BWRs currently shut down in Japan, it will bring great benefits because the system uses fission chambers installed inside the reactor vessel.

7. Conclusion

Until now, alpha decay pulses were not used for practical applications because the pulse heights were either too small to observe, or they were thought to be mixed in with white noise. However, we were able to observe the pulse signals generated by the spontaneous alpha decay of uranium coated on the electrodes of fission chambers in the LHD of NIFS. These alpha decay pulses can be applied to new and improved investigation methods for fission detectors and preamplifiers in ITER and JT-60SA. Using alpha decay signals is also helpful in meeting the ALARA policy in terms of not having to use radiation sources and can be beneficial for verifying the health of systems having fission chambers, in both fusion facilities and fission reactors.

Acknowledgments

This work was performed with the support and under the auspices of the QST Collaboration Research Program and the NIFS Collaboration Research Program (NIFS22KIEH003).

- [1] M. Ishikawa *et al.*, Fusion Eng. Des. **109-111, Part B**, 1399 (2016).
- [2] G.F. Knoll, *Radiation Detection and Measurement, 4th ed.*, (Wiley, New York, 2010), p.134, p.538.
- [3] M. Isobe *et al.*, Rev. Sci. Instrum. **85**, 11E114 (2014).
- [4] M. Isobe *et al.*, IEEE Trans. Nucl. Sci. **46**, No.6, 2050 (2018).
- [5] D. Ito *et al.*, Plasma Fusion Res. **16**, 1405018 (2021).
- [6] J. Kinoshita *et al.*, PNC-TJ201 73-02 (1973) [in Japanese].
- [7] N. Wakayama, JAERI-M 85-193 (1985) [in Japanese].
- [8] *Radioisotope Pocket Data Book, 12th ed.*, JRIA, (Maruzen, Tokyo, 2020) [in Japanese].
- [9] J.M. Alexander and M.F. Gazdik, Phys. Rev. **120**, 874 (1960).
- [10] *Average Energy Required to Produce an Ion Pair*, ICRU Report 31, (ICRU, Washington, DC, 1979).
- [11] P. Filliatre *et al.*, Nucl. Instrum. Methods Phys. A **817**, 1 (2016).
- [12] N. Wakayama *et al.*, JAERI-12697 (1967) [in Japanese].
- [13] H.A. Bethe, USAEC Doc. BNL-T-7 (1949).